Laser Coherent Combination With Circular Array of Airy Beams

Huahua Wang, Yang Liu, Jian Ma, Qin Wen, Xingwang Kang, Haoran Du, Xinglin Zhong, Fei Chen, Junjie Sun, Lu Gao, and Ze Zhang

***Abstract*—A high-efficiency laser coherent combination method based on the virtue of the self-transverse acceleration effect of Airy beams is proposed and demonstrated by converting an array of Gaussian beams into Airy beams array to reduce laser beams separation distance. The coherent combination procedures of circular array for both Airy and Gaussian beams are theoretically and experimentally studied. The results show that the central intensity of the laser coherent combination of the circular array of Airy beams is 14.33 times higher than that of the Gaussian beams array, and the combined efficiency of the circular array of Airy beams is 1.64 times higher than that of the Gaussian beams circular array. The method may provide an efficient way to increase combination efficiency of laser coherent combination array and may have a broad application prospect in optical communication, particle capture, material processing.**

***Index Terms*—Airy beam, circular array, coherent combination, filling factor, self-transverse acceleration effect.**

Manuscript received 12 September 2023; revised 5 November 2023; accepted 15 November 2023. Date of publication 29 November 2023; date of current version 26 December 2023. This work was supported in part by the National Natural Science Foundation of China under Grants 12074350 and 62105341, in part by the Fundamental Research Funds for the Central Universities under Grants 265202046 and 590122050, in part by the National Science Foundation of Shandong Province, China under Grant ZR2021QF126, in part by Innovative Cross Team of the Chinese Academy of Sciences under Grant JCTD-2020-13, and in part by the Science and Technology on Solid–State Laser Laboratory Stability Support Project. *(Corresponding authors: Ze Zhang; Lu Gao; Yang Liu.)*

Huahua Wang and Lu Gao are with the Aerospace Information Research Institute, Chinese Academy of Sciences, Beijing 100045, China, and also with the School of Science, China University of Geosciences, Beijing 100190, China (e-mail: gaolu@cugb.edu.cn).

Yang Liu, Qin Wen, and Xingwang Kang are with the Aerospace Information Research Institute, Chinese Academy of Sciences, Beijing 100045, China (e-mail: liuyang01@aircas.ac.cn).

Jian Ma and Haoran Du are with the School of Science, China University of Geosciences, Beijing 100190, China.

Xinglin Zhong is with the School of Eletronic Engineering, Beijing University of Posts and Telecommunications, Beijing 100876, China.

Fei Chen is with the Changchun Institute of Optics, Fine Mechanics and Physics, Chinese Academy of Sciences, Changchun, Jilin 130022, China.

Junjie Sun is with the Changchun Institute of Optics, Fine Mechanics and Physics, Chinese Academy of Sciences, Changchun, Jilin 130022, China, and also with the University of Chinese Academy of Sciences, Beijing 101408, China.

Ze Zhang is with the Aerospace Information Research Institute, Chinese Academy of Sciences, Beijing 100045, China, also with the Key Laboratory of Computational Optical Imaging Technology, Chinese Academy of Sciences, Beijing 100094, China, and also with the School of Eletronic Engineering, Beijing University of Posts and Telecommunications, Beijing 100876, China (e-mail: zhangze@aoe.ac.cn).

Digital Object Identifier 10.1109/JPHOT.2023.3335099

I. Introduction

HIGH-POWER laser is always desired in many applications, such as free space laser communication, laser cutting and welding, or even laser weapon system [1], [2], [3]. However, due to thermal and nonlinear effect, it is usually very difficult to realize high power output for a single laser system. For decades, laser coherent combination has been proved to be an efficient way to combine multiple laser beams together for achieving high power output due to its advantage of maintaining good beam quality. And many studies have demonstrated filling factor [4], [5], [6] is an important parameter to affect coherent combination efficiency [7], [8], [9]. To increase beam coherent combination, people need to reduce beams space and increase the filling factor of coherent combination array.

Up to now, the transmission-type and reflection-type structures are mainly coherent combination techniques to increase the filling factor. Numerous studies have shown that people are more adopting transmission-type structure because the optical elements in the reflection-type system are scattered and the scalability is not strong [9], [10], [11]. In 2014, Tan et al. achieved a multi-intersection array of wavelength size by means of tight focusing [12]. The Thales Group of France theoretically realized coherent beam combining of 60 femtosecond fiber amplifiers by numerical simulation with programmable algorithms [13]. In addition, Geng et al. successively carried out the 7-beam coherent combination with a sub-aperture diameter of 28 mm and adjacent sub-aperture spacings of 42 mm and 32 mm by using a 7-unit high-duty ratio fiber collimator in 2021 and 2022 [14], [15]. The transmission coherent combination technique has a compact structure and good scalability, which demonstrates a good application prospect in military fields such as laser weapons in recent years. However, due to the limitation of the filling factor of the laser array, it is difficult to further improve the beam quality beyond the diffraction limit.

In this paper, we report a coherent combination method by converting Gaussian beams array to Airy beams array. By the virtue of self-transverse acceleration effect [16], [17], [18], [19], all Airy beams bend towards center so that their beams separation distance could be reduced and thus the filling factor is increased during propagation. This method, which has a simple structure, can be expanded into a large array of thousands of beams, and also has more precise position compared to a tiled array. The propagation characteristics and coherent combination efficiency of circular array of Airy beams combination beams

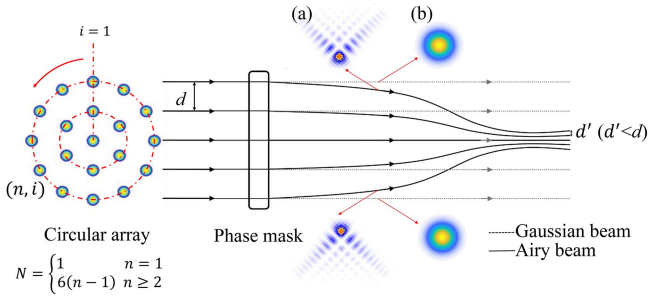

Fig. 1. Schematic diagram of circular array of Airy beams generated by phase mask modulation. (a) represents the intensity distribution of 2D Airy beam spot; (b) represents the intensity distribution of Gaussian beam spot.

are studied both theoretically and experimentally. Compared with traditional method of using Gaussian beams, our method shows higher central intensity and better coherent combination efficiency.

II. Theoretical Analysis

The mechanism for highly efficient generation of circular array of Airy beams through a phase mask can be understood intuitively from Fig. 1. The insets (a) and (b) represent the intensity distribution of 2D Airy beam and the intensity distribution of Gaussian beam, respectively.

The sub-beams of the input Gaussian beam arranging in a ring around the center are modulated by a phase mask into many truncated Airy beams. In the initial state, the distance between two adjacent beams in the radial direction is d, and then the distance decreases d' with the beams bend toward the center because of the self-acceleration effect after modulated by the diaphragm. Therefore, the filling factor of the beam array can be improved. Each of wave components with Airy-type phase modulation propagates along curved trajectory. It is obvious that the transverse wave-vectors can be cancelled for radially symmetric beams on the same ring. Consequently, the combination beam can maintain stable transmission in a certain range. The detailed theoretical explanations are shown below.

The electric field of the Airy sub-beams in the initial plane z = 0 of the Cartesian coordinate system is designed as [20], [21]:

$$E(x,y,0) = A\exp\left(\frac{aX_{n,i}}{\omega_0}\right)Ai\left(\frac{X_{n,i}}{\omega_0}\right)\exp\left(\frac{aY_{n,i}}{\omega_0}\right)Ai\left(\frac{Y_{n,i}}{\omega_0}\right), \tag{1}$$

where $Ai(\cdot)$ represents the Airy function, $X_{n,i} = x + x_{n,i}$ and $Y_{n,i} = y + y_{n,i}$. x and y are two transverse coordinates, respectively. $x_{n,i}, y_{n,i}$ is the center position coordinate of the sub-beam and it is determined by that distance of the sub-beam off the central optical axis, where n denotes the number of rings in the circle array, i is the count number of sub-beam in the ring. z-axis is the longitudinal coordinate and is consistent with the beam propagation direction. $0 < a \leq 1$ is an exponential decay factor and w_0 is a constant governing the size of the Airy sub-beam. A is a real constant and ensures that the maximum light intensity in the initial plane I_0 is always 1. The electric field of the Airy beams propagating in free space is described as [22], [23]:

$$\begin{aligned} &E(x,y,z) \\ &= \frac{k}{j2\pi z}\iint_{-\infty}^{\infty}\exp\left\{\frac{jk}{2z}\left[(x-x')^2+(y-y')^2\right]\right\}dx'dy' \\ &= E(x,z)E(y,z), \end{aligned} \tag{2}$$

where $k = 2\pi/\lambda$ with λ being the wavelength and j is an imaginary unit. To understand the influence of these phase modulation, let us first consider the one-dimensional domain case of $E(x,z)$. $E(x,z)$ can be written as:

$$\begin{aligned} E(x,z) = &\sqrt{\frac{Ak}{j2\pi z}}\int_{-\infty}^{\infty}\exp\left(\frac{aX_{n,i}}{\omega_0}\right)Ai\left(\frac{X_{n,i}}{\omega_0}\right) \\ &\times\exp\left\{\frac{jk}{2z}\left[(x-x')^2\right]\right\}dx'. \end{aligned} \tag{3}$$

We find that the Airy beam evolves can be analytically given as:

$$\begin{aligned} &E(x,z) \\ &= Ai\left[\frac{aX_{n,i}}{\omega_0} - \left(\frac{z}{2k\omega_0^2}\right)^2 + ja\frac{z}{k\omega_0^2}\right] \\ &\quad\times\exp\left[\frac{aX_{n,i}}{\omega_0} - \frac{a}{2}\left(\frac{z}{k\omega_0^2}\right)^2 - j\frac{(z/k\omega_0^2)^3}{12} + j\frac{za^2}{2k\omega_0^2}\right] \\ &\quad\times\exp\left[j\frac{X_{n,i}}{\omega_0}\frac{z}{2k\omega_0^2}\right]. \end{aligned} \tag{4}$$

By using the same expression as above, the analytical expression of *E(y, z)* turns out to be

$$\begin{aligned} &E(y,z) \\ &= Ai\left[\frac{aY_{n,i}}{\omega_0} - \left(\frac{z}{2k\omega_0^2}\right)^2 + ja\frac{z}{k\omega_0^2}\right] \\ &\quad\times\exp\left[\frac{aY_{n,i}}{\omega_0} - \frac{a}{2}\left(\frac{z}{k\omega_0^2}\right)^2 - j\frac{(z/k\omega_0^2)^3}{12} + j\frac{za^2}{2k\omega_0^2}\right] \\ &\quad\times\exp\left[j\frac{Y_{n,i}}{\omega_0}\frac{z}{2k\omega_0^2}\right] \end{aligned} \tag{5}$$

From the argument of the Airy function in (4) and (5), one can conclude that main lobe beam of this sub-beam follows a trajectory in the X–z and Y-z plane described by the curve $X = z^2/4\,k^2 w_0^3 a$. The trajectory of the beam intensity features is the parabolic deflection proportional to the propagation distance in the physical units. The corresponding Newtonian (kinematical) equations describing these trajectories are $d^2X/dz^2 = 1/2\,k^2 w_0^3 a = g$ and $dX/dz = gz$. The wave will follow a parabolic trajectory and the wave packet will decelerate downwards. Using the analysis of the reference [24] we study the motion of the center of gravity of these finite energy Airy wave packets. As usual, the intensity centroid is defined as $\langle X\rangle = \int X|\Psi(X,z)|^2 dX/N$, where in our case the constant norm N is given by $N = \int|\Psi(X,z)|^2 dX$ [17], [25]. Fig. 2

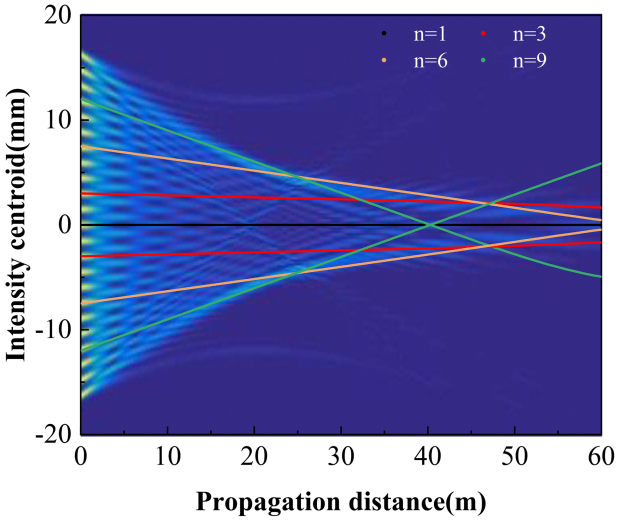

Fig. 2. Trajectories of sub-beam intensity centroid.

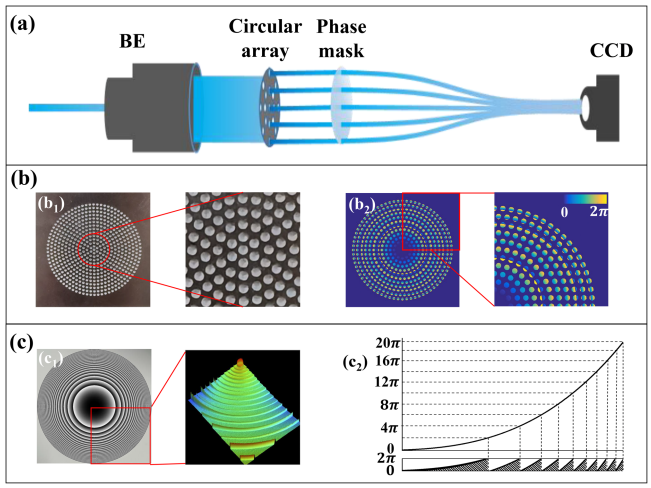

Fig. 3. (a) Experimental diagram of circular array of Airy beams. (b) The array with circular arranged through holes (b_1) and the phase structure (b_2). (c) The phase mask for modulation of the circular beam array (c_1) and the phase distribution structure (c_2) of phase mask.

clearly shows the trajectories of sub-beam intensity centroid. We can see that with the increase of n, the beam converges to the central optical axis faster and the spacing between sub-beams decreases, as well as the beam energy involved in coherent combination also increases. The results indicate that each Airy beam of radial symmetry converges toward the central axis, therefore the separation distance between the beams is reduced. And the filling factor of the circular array in the cross-section over each specific transmission distance increases due to the reduced distance between the sub-beams. It can also enable the peripheral sub-beams far away from the center to participate in the coherent combination process more effectively. At the same time, the stronger coherence between each of them can be ensured in the transmission of long distance, and finally the coherent combined beam of the Airy beam array can have higher energy and more stable transmission.

III. Experimental Setup

The experimental diagram to generate Airy beams circular array is shown in Fig. 3(a). The Gaussian light (Coherent, Genesis CX480-4000) with a wavelength of 480 nm and a beam waist radius of 1 mm is collimated and magnified 20 times by a beam expander (BE). Then it is truncated by a metal mask with a size of 50 mm $\times$ 50 mm and a thickness of 1 mm to produce a circular array, which is composed of 469 circular apertures with a radius of 0.5 mm and 1.5 mm between adjacent apertures. The circular array and phase structure array are shown in Fig. 3(b). The Gaussian beams circular array is modulated into an Airy circular array by the phase mask. Finally, the beam transverse structure at different positions is monitored by moving the beam analyzer (Jingili Optoelectronics).

In particular, the phase mask we designed is shown in Fig. 3(c) with a phase depth of 20π. To reduce the thickness and processing difficulty of the diaphragm, the phase folding technique is used to optimize the cubic phase into 10 concentric rings structure with same phase depth of 2π, and a step height of each ring is 40 nm [18], [26], [27]. The right subgraph in Fig. 3(c) shows the cubic phase curve of a diaphragm with 10 phase depths.

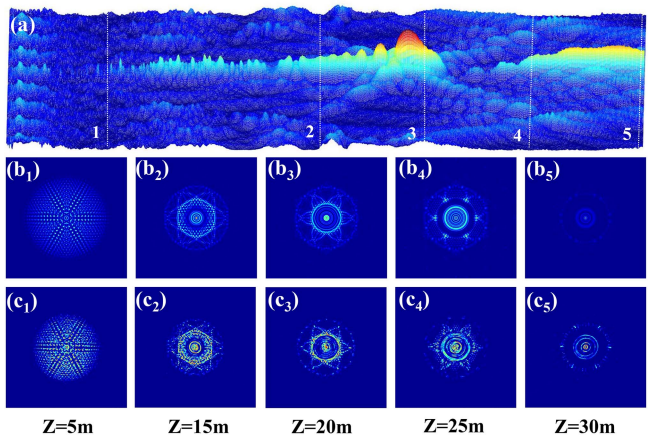

Fig. 4. Numerical and experimental results of coherent combination of circular array of Airy beams. (a): Side-view of the beam of 30-meter propagation numerically retrieved from the phase mask. $(b_1)-(b_5)$: Snapshots of transverse intensity patterns of the beam at planes 1-5 marked in (a). $(c_1)-(c_5)$: Experimental results corresponding to $(b_1)-(b_5)$.

IV. Experimental Results and Analysis

The experimental results are shown in Fig. 4, where (a) displays the numerical longitudinal beam structure traveling through 30 meters. Snapshots of the transverse intensity patterns at positions from 1 to 5, which are at the distances of 5 m, 15 m, 20 m, 25 m and 30 m, respectively. The corresponding experimental profiles are shown in Fig. 4(b_1–b_5) and (c_1–c_5). Our experimental results agree well with the numerical simulations in all cases. It can be seen that as the distance increases, the spot size becomes smaller and the energy converges towards the

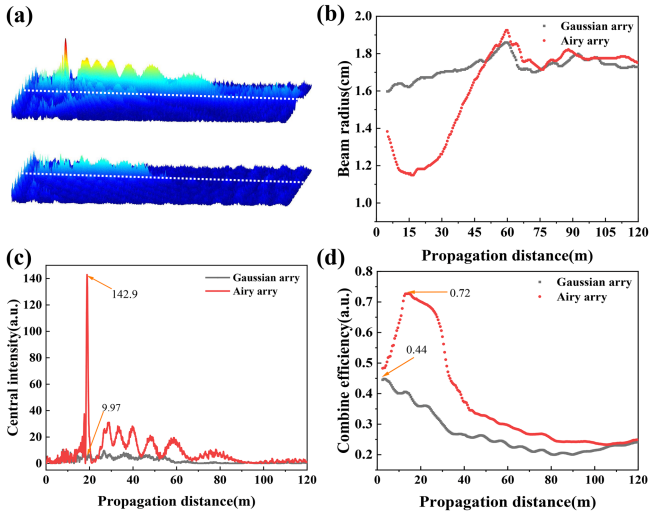

Fig. 5. Comparison between the experimental results of the Gaussian and Airy circular array beams. (a) Side-view of the beam of 120-meter propagation numerically retrieved of the Airy (up) and Gaussian beams circular array (down) from the phase mask. (b) The beam radius of the Gaussian and Airy beams circular array versus the propagation distance with the power ratio of 84%. (c) The transmission intensity curve diagram along the central axis with the propagation distance of 120 meters. (d) The combination efficiency of the Gaussian and Airy beams circular array versus the propagation distance propagation distance when the bucket power ratio radius is 0.75 cm.

central axis, and the stable transmission of high energy can be maintained.

In order to effectively evaluate the coherent combination quality of the circular array of Airy beams, we analyzed the energy distribution from the target spot by using two comparison methods of power in the bucket (PIB) [24], [28]. The comparison results are shown in Fig. 5. The inset (a) represents the side-view of the beam of 120-meter propagation numerically retrieved of the Airy (up) and Gaussian beams circular array (down) from the phase mask. The inset (c) represents the transmission intensity curve diagram along the central axis with the propagation distance of 120 m. From Fig. 5(c), we can calculate that the central intensity of the laser coherent combination of the circular array of Airy beams is 14.33 times higher than that of the Gaussian beams. In the first comparison method of PIB, we fixed the ratio of the energy in the bucket to the total energy of the target spot. The fixed ration is 84%, then the bucket radius satisfying this ratio is calculated, as shown in Fig. 5(b). The black dots and red dots are the simulation fitting curves of the Gaussian beam array and Airy beam array, respectively. It can be seen that the bucket radius of Airy beam array is always smaller than that of the Gaussian beam array under the first 60 m propagation distance, and the difference is not significant after 60 m.

In another comparison method of PIB, we fixed the bucket radius 0.75 cm. Then the ratio of the energy in the fixed bucket to the total energy of the target spot can be calculated, as shown in Fig. 5(d). It is obvious that the coherent combination efficiency of the Airy beam array is always higher than that of the Gaussian beam array in the scope of the detection distance, and the combined efficiency of the circular array of Airy beams is 1.64 times higher than that of the Gaussian beams circuar array. The experimental results in Fig. 5 show that the coherent combination efficiency of Airy beam array is always better, and the energy of coherent combination beams is also more concentrated. The coherent combination beam of Airy beam array can maintain long-distance transmission with high-energy.

V. Conclusion

According to the basic principle of coherent combination, a method to improve the filling factor of beam array by using the transverse self-acceleration property of Airy beam is proposed in this paper. The results of simulation indicate that the coherent combination beam of circular array of Airy beams has higher energy, better quality and longer stable transmission distance. In the experiment, the circular array of Airy beams is obtained by using the metal sheet and phase mask. The experimental results further verify the improvement of circular array of Airy beams in terms of beam quality, energy and shape retention in coherent combination. This beam combination method has great application prospects in improving the distance of spatial optical communication, laser cutting efficiency, improving the power of high-energy laser.

References

[1] G. Mourou, B. Brocklesby, T. Tajima, and J. Limpert, "The future is fibre accelerators," *Nature Photon.*, vol. 7, pp. 258–261, Mar. 2013.
[2] T. Fan, "Laser beam combining for high-power, high-radiance sources," *IEEE J. Sel. Topics Quantum Electron.*, vol. 11, no. 3, pp. 567–577, May/Jun. 2005.
[3] T. J. Wagner, "Fiber laser beam combining and power scaling progress: Air force research laboratory laser division," *Proc. SPIE*, vol. 8237, 2012, Art. no. 823718.
[4] G. D. Goodno and J. E. Rothenberg, *Engineering of coherently combined, high-power laser systems*. Hoboken, NJ, USA: John Wiley and Sons Ltd, 2013, pp. 1–44.
[5] M. A. Vorontsov, T. Weyrauch, L. A. Beresnev, G. W. Carhart, L. Liu, and K. Aschenbach, "Adaptive array of phase-locked fiber collimators: Analysis and experimental demonstration," *IEEE J. Sel. Topics Quantum Electron.*, vol. 15, no. 2, pp. 269–280, Mar./Apr. 2009.
[6] G. D. Goodno et al., "Coherent combination of high-power, zigzag slab lasers," *Opt. Lett.*, vol. 31, no. 9, pp. 1247–1249, May 2006.
[7] R. Uberna, A. Bratcher, and B. G. Tiemann, "Coherent polarization beam combination," *IEEE J. Quantum Electron.*, vol. 46, no. 8, pp. 1191–1196, Aug. 2010.
[8] N. Siahvashi, M. Hamdami, A. Arabanian, and R. Massudi, "Increasing the power and quality of beam in coherent combination of laser beams by controlling optical axis angles," *Opt. Quantum Electron.*, vol. 53, pp. 1–15, 2021.
[9] Z. Liu, X. Jin, R. Su, P. Ma, and P. Zhou, "Development status of high power fiber lasers and their coherent beam combination," *Sci. China Inf. Sci.*, vol. 62, pp. 1–32, 2019.
[10] B. Liu, Y. Liu, and Y. Braiman, "Coherent addition of high power laser diode array with a V-shape external talbot cavity," *Opt. Exp.*, vol. 16, no. 25, pp. 20935–20942, Dec. 2008.
[11] X. Fan, J. Liu, J. Liu, and J. Wu, "Coherent combining of a seven-element hexagonal fiber array," *Opt. Laser Technol.*, vol. 42, no. 2, pp. 274–279, 2010.
[12] Y. Tan and X. Li, "Influence of filling factor on far-field intensity distribution in coherent beam combination," *Acta Physica Sinica*, vol. 63, no. 2, p. 094202, 2014.
[13] F. Ihsan et al., "Coherent beam combining of 61 femtosecond fiber amplifiers," *Opt. Exp.*, vol. 28, pp. 20152–20161, 2020.
[14] C. Geng et al., "Experimental demonstration of adaptive optics correction of the external aberrations for distributed fiber laser array," *IEEE Access*, vol. 9, pp. 51464–51472, 2021.

[15] X. Yang et al., "Continuous tracking and pointing of coherent beam combining system via target-in-the-loop concept," *IEEE Photon. Technol. Lett.*, vol. 33, no. 20, pp. 1119–1122, Oct. 2021.
[16] G. A. Siviloglou, J. Broky, A. Dogariu, and D. N. Christodoulides, "Observation of accelerating airy beams," *Phys. Rev. Lett.*, vol. 99, 2007, Art. no. 213901.
[17] G. A. Siviloglou and D. N. Christodoulides, "Accelerating finite energy airy beams," *Opt. Lett.*, vol. 32, no. 8, pp. 979–981, Apr. 2007.
[18] Z. Zhang et al., "Robust propagation of pin-like optical beam through atmospheric turbulence," *APL Photon.*, vol. 4, no. 7, 2019, Art. no. 076103.
[19] P. Zhang et al., "Trapping and guiding microparticles with morphing autofocusing airy beams," *Opt. Lett.*, vol. 36, pp. 2883–2885, 2011.
[20] Y. Hu, G. A. Siviloglou, P. Zhang, N. K. Efremidis, D. N. Christodoulides, and Z. Chen, *Self-Accelerating Airy Beams: Generation, Control, and Applications*. New York, NY, USA:Springer, 2012.
[21] N. K. Efremidis, Z. Chen, M. Segev, and D. N. Christodoulides, "Airy beams and accelerating waves: An overview of recent advances," *Optica*, vol. 6, no. 5, pp. 686–701, May 2019.
[22] S. A. Collins, "Lens-system diffraction integral written in terms of matrix optics," *J. Opt. Soc. America*, vol. 60, pp. 1168–1177, 1970.
[23] Y. Zhou, X. Zang, W. Dan, F. Wang, R. Chen, and G. Zhou, "Design and realization of an autofocusing airyprime beams array," *Opt. Laser Technol.*, vol. 162, 2023, Art. no. 109303.
[24] Y. P. Wang, J. Y. Huang, and G. L. Qiao, "A method for evaluating high energy laser beam quality," *J. Optoelectronics Laser*, vol. 12, no. 10, pp. 1029–1033, 2001.
[25] G. A. Siviloglou, J. Broky, A. Dogariu, and D. N. Christodoulides, "Ballistic dynamics of airy beams," *Opt. Lett.*, vol. 33, no. 3, pp. 207–209, Feb. 2008.
[26] D. Bongiovanni et al., "Free-space realization of tunable pin-like optical vortex beams," *Photon. Res.*, vol. 9, no. 7, pp. 1204–1212, Jul. 2021.
[27] S. Droulias, M. Loulakis, D. G. Papazoglou, S. Tzortzakis, Z. Chen, and N. K. Efremidis, "Inverted pin beams for robust long-range propagation through atmospheric turbulence," *Opt. Lett.*, vol. 48, pp. 5467–5470, 2023.
[28] Z. Cheng, X. Li, J. Jiang, G. Xu, H. Shi, and J. Xia, "Focus characteristics of laser beam for long-distance propagation in atmosphere," *Proc. SPIE*, vol. 21, pp. 533–543, 2000.